Supplemental Data

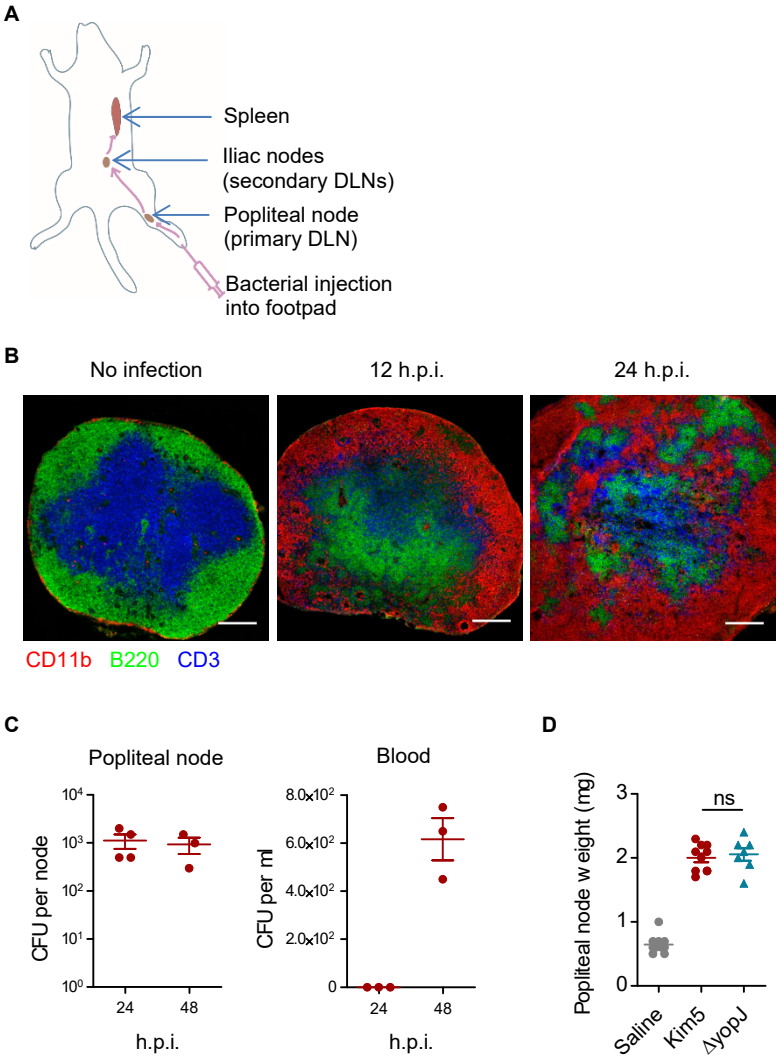

Supplemental Figure 1. Bubo formation precedes systemic infection. (**A**) The footpad infection model: bacteria injected in a rear footpad encounter a single sentinel draining node (popliteal node, PN) before reaching secondary nodes (iliac nodes, INs) and beyond. (**B**) PN tissue sections harvested from mice injected in footpad with saline, Kim5 or Δ*yopJ* bacteria; and stained for B cells (B220, green), T cells (CD3, blue) and $CD11b^{+}$ cells (red); scale bar, 200 μm. (**C**) Count of viable bacteria from PNs and blood at indicated time points post footpad infection (n = 3-4). (**D**) Weight of the PNs harvested 24 h.p.i. (n = 7-10). Data were analyzed via one-way ANOVA; ns, not significant.

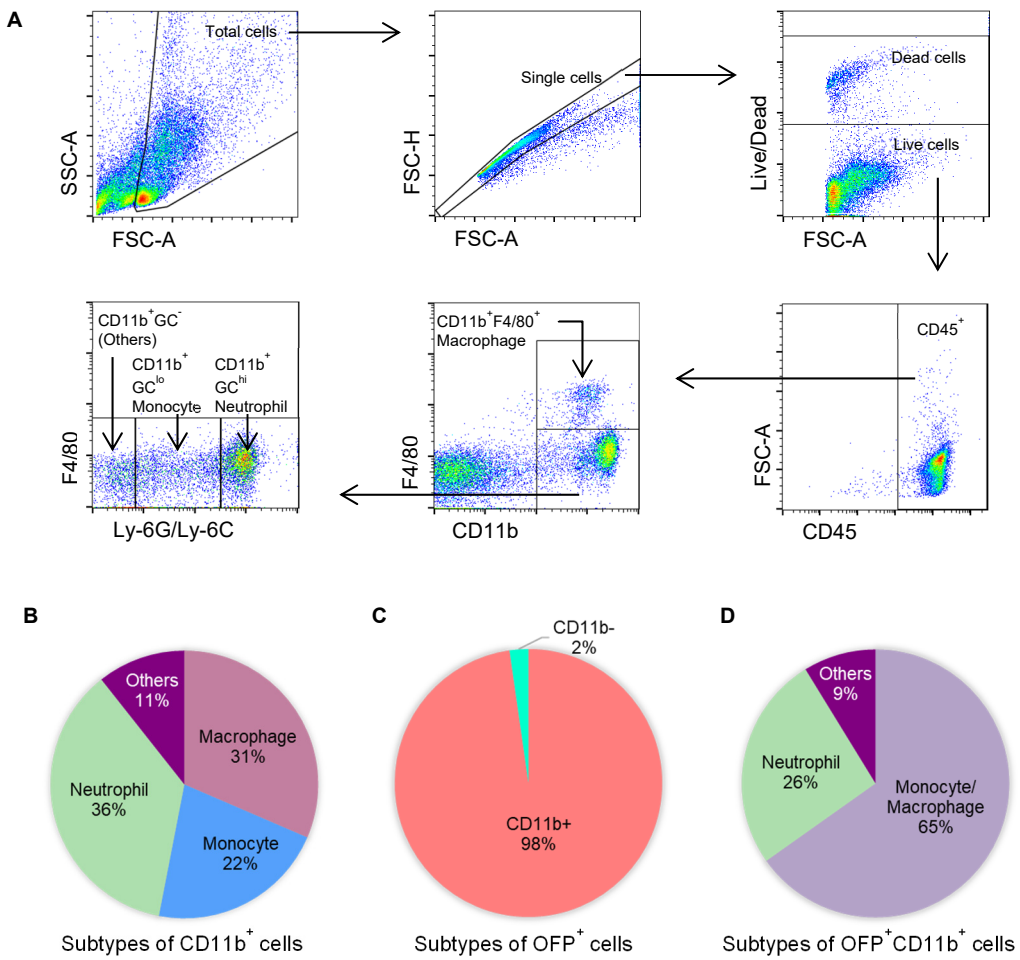

Supplemental Figure 2. Monocytes/macrophages are major targets of *Y. pestis* in buboes. (**A**) Flow cytometry gating strategy. Ly-6GC^{hi} cells detected by an anti-Ly-6G and Ly-6C antibody (Clone RB6-8C5) were defined as neutrophils (further verified as Ly6G^{hi} using anti-Ly-6G antibody clone 1A8, data not shown) and Ly-6GC^{lo} cells as monocytes (further verified as Ly6C^{hi} using anti-Ly-6C antibody clone AL-21, data not shown). 'Others' indicate residual CD11b^{+} cells, which include mostly NK cells and dendritic cells, were not subtyped in these samples. (**B**) Mean percentage of major phagocytic cell types as a proportion of total CD11b^{+} cells in PNs 24 h.p.i. with *Y. pestis* Kim5 (n = 9). (**C**) Mean percentage of CD11b^{+} cells as a proportion of total OFP^{+} cells in PNs (n = 4). (**D**) Mean percentage of major phagocytic cell types as a proportion of total OFP^{+} cells in PNs (n = 4).

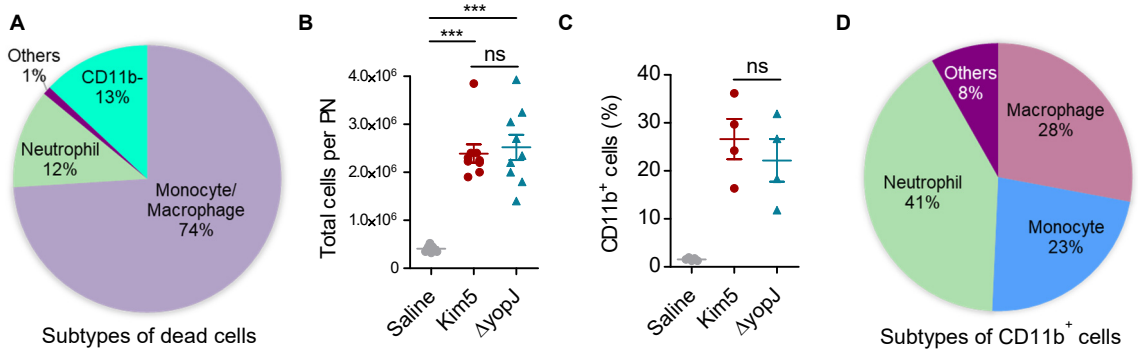

1

2 **Supplemental Figure 3. Cellular infiltration in buboes is independent of macrophage death.** (**A**)
3 Percentage of various cell types as a proportion of total dead cells in single cell suspensions prepared
4 from PNs 24 hours post footpad infection with Kim5 bacteria. (**B and C**) Total number of cells (**B**) and
5 percentage of $CD11b^+$ cells (**C**) in PNs, 24 h.p.i. (n = 7-9). (**D**) Mean percentage of major phagocytic cell
6 types as a proportion of total $CD11b^+$ cells in PNs 24 h.p.i. with Δ*yopJ* strain (n = 9). Data were analyzed
7 via one-way ANOVA. ***p<0.001; ns, not significant.

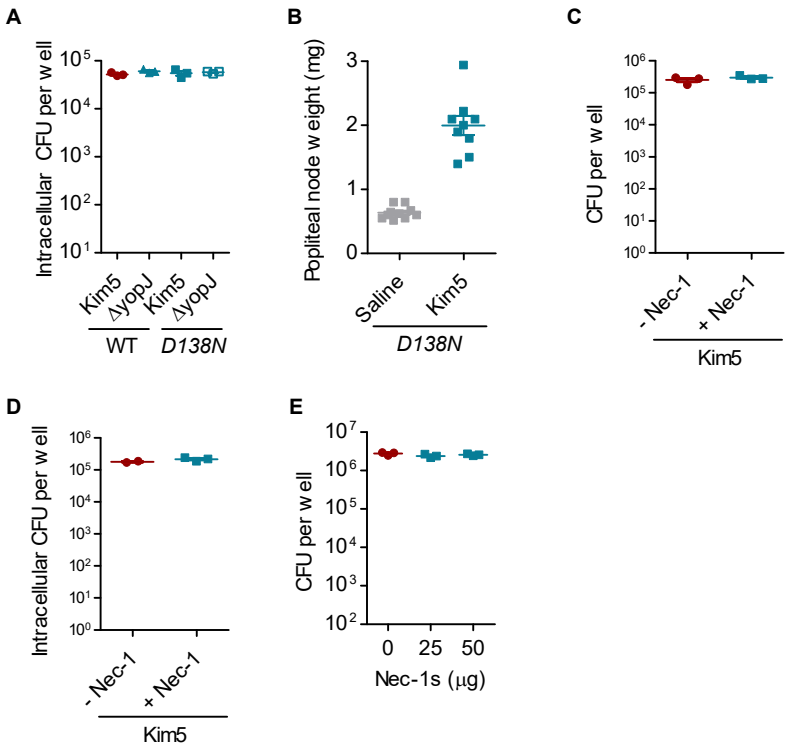

Supplemental Figure 4. Macrophage phagocytosis and bubo formation are independent of RIPK1 kinase activity. (**A**) Number of intracellular bacteria per well as determined by CFU counts. 2 x 10^4 BMMΦs from WT or *Ripk1*$^{D138N/D138N}$ mice were infected with bacteria at MOI 10 for 2 hours, treated with gentamicin for an hour, then washed, lysed and plated (n = 3). (**B**) PN weights of *Ripk1*$^{D138N/D138N}$ mice 24 hours post footpad injection with saline or Kim5 bacteria (n = 9-10). (**C**) Number of viable bacteria per well determined by agar plating. 2 x 10^5 bacteria were incubated for 2 hours with media alone or media containing Nec-1 and then plated for CFU count Number of viable bacteria per well determined by agar plating. 2 x 10^5 bacteria were incubated for 2 hours with media alone or media containing Nec-1 and then plated for CFU count (n = 3). (**D**) Number of intracellular bacteria per well. 2 x 10^5 macrophages were pre-incubated with or without Nec-1 for 2 hours, infected with bacteria (MOI 10) for 30 min and treated with gentamicin for an hour in presence or absence of Nec-1, then washed, lysed and plated for CFU count (n = 2-3). (**E**) Number of viable bacteria per well determined by agar plating. 10^5 bacteria were incubated for 24 h with media alone or media containing indicated amount of Nec-1s and then plated for CFU count (n = 3).

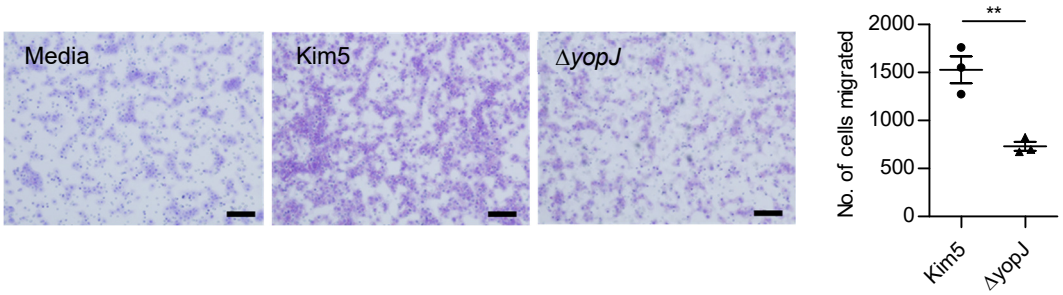

Supplemental Figure 5. YopJ-triggered cell death results in chemotaxis of uninfected macrophages. Representative images of trans-well migration of J774A.1 cells towards uninfected, Kim5-infected or Δ*yopJ*-infected cells. Images of the filter membranes were taken after fixation and staining of cells migrated across the membrane (purple in color) as described in the methods. Scale bar, 200 μm. Pores of the membranes are also visible in the images as the numerous small, round dots. Graph shows quantification of migrated cells (n = 3). Data were analyzed via unpaired two-tailed Student's t test, **p <0.01.

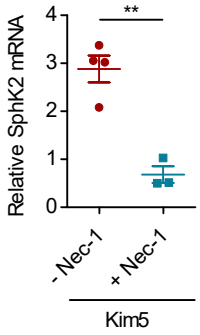

Supplemental Figure 6. *Sphk2* expression in *Y. pestis*-infected macrophages is dependent on RIPK1 kinase activity. Relative *Sphk2* mRNA expression in Kim5-infected macrophages in presence or absence of Nec-1 (n = 3-4). Data were analyzed via unpaired two-tailed Student's t test, **p <0.01.

Supplemental Video Legends

Supplemental Video 1. Bacterial release from a *Y. pestis*-infected cell in vitro.

Video depicting intracellular replication of Kim5-OFP bacteria followed by their extracellular release and infection of neighboring cells. The bacteria are shown in red. Timestamp indicates hh:mm.

Supplemental Video 2. Absence of bacterial release from a Δ*yopJ*-infected cell in vitro.

Video depicting intracellular replication but no bacterial release from a cell infected with Δ*yopJ*-OFP bacteria. The bacteria are shown in red. Timestamp indicates hh:mm.

Supplemental Video 3. Cell lysis during *Y. pestis* infection in vitro.

Video depicting lysis of an initially Kim5-infected cell followed by lysis of neighboring cells over time. The initially infected cell is shown in green (which faded eventually) and indicated by the arrow. Lysed cells are shown in red. Timestamp indicates hh:mm.